MODIFICATION OF THE SSG/LRR-ω RSM FOR ADVERSE PRESSURE GRADIENTS USING TURBULENT BOUNDARY LAYER EXPERIMENTS AT HIGH Re

T. Knopp[1], M. Novara[1], D. Schanz[1], N. Reuther[3], W. Lühder[1], C. Willert[2], A. Schröder[1], E. Schülein[1], R. Hain[3], and C. J. Kähler[3]

[1] *Institute of Aerodynamics and Flow Technology, DLR, Göttingen, Germany*

[2] *Institute of Propulsion Technology, DLR, Köln, Germany*

[3] *Institute of Fluid Mechanics and Aerodynamics, Universität der Bundeswehr München, Germany*

Tobias.Knopp@dlr.de

Abstract

A modification of the SSG/LRR-ω model for turbulent boundary layers in adverse pressure gradient is presented. The modification is based on a new wall law for the mean velocity at adverse pressure gradient. The wall law is found from two new joint DLR/UniBw experiments and from the analysis of a data base from the literature. The mean velocity profile in the inner layer is found to consist of a log-law region, which is thinner than its zero pressure gradient counterpart, and a half-power law region above the log law. An empirical correlation for the wall-distance of the transition from the log-law to the half-power law is presented. Then a modification of the ω-equation to account for a half-power law behaviour of the mean velocity is described. The modified SSG/LRR-ω model is then applied to the two joint DLR/UniBw experiments. The modification leads to a reduction of the mean velocity in the inner part of the boundary layer and makes the model more susceptible for flow separation, which is in good agreement with the experimental data.

1 Introduction

The numerical prediction of separation of a turbulent boundary layer on a smooth surface due to an adverse-pressure gradient (APG) in the low-speed regime is of fundamental importance for many technical applications, e.g. the flow around aircraft wings during take-off and landing. However, there is still no consensus in the research literature on the existence of a wall-law for the mean-velocity profile at adverse pressure gradients, which only depends on local flow parameters, see e.g. Alving and Fernholz (1995), Johnstone et al. (2010). The knowledge of a wall law could be used to improve RANS turbulence models. There has been a noticeable research activity on turbulent boundary layer flows in adverse pressure gradient during the last decade. New experimental studies, e.g. by Schatzman and Thomas (2017), and from direct numerical simulations (DNS) by Coleman et al. (2018) have been performed during the last years. The interest in RANS turbulence modelling for flow separation is also apparent from the memoranda by Slotnick et al. (2014) and Bush et al. (2019).

The number of well-defined and documented validation test cases at high Re is still small in the literature. Therefore, since 2011 a series of three new boundary-layer experiments were designed and performed in a joint work by DLR and the Universität der Bundeswehr München (UniBw), funded mainly within the DLR aeronautical program and in parts by DFG. The first experiment was at moderately large Reynolds numbers up to $Re_\theta = 10000$ of the incoming boundary layer before entering the APG region, see Knopp et al. (2014a). The DLR/UniBw exp. II was performed at higher Reynolds numbers up to $Re_\theta = 30000$ of the incoming boundary layer. The adverse-pressure gradient was moderately strong and the flow was remote from separation, see Knopp et al. (2021). The DLR/UniBw exp. III was at a strong adverse-pressure gradient, causing flow separation and a thin separation bubble, see Knopp et al. (2018).

The goals of the experiments were to establish a data base for the mean velocity at APG, and to provide a new well-defined and documented test case for the validation of RANS and hybrid RANS/LES methods at APG.

The great question is the existence of a wall-law for the mean velocity in the inner layer, which depends only on local flow parameters. The present work is based on the following ideas. The first idea is that there still exists a logarithmic region under APG conditions, which becomes smaller as the flow approaches separation, see Alving and Fernholz (1995), and Knopp et al. (2021). The second idea is that there is a systematic reduction of the extent of the log-law region at APG, see Knopp (2016), which was found for Couette-Poisseuille flow by Telbany and Reynolds (1980). The next idea follows Perry et al. (1966), who proposed that, above the log-law, a half-power law (or square-root law) emerges, extending to the wall distance the log-law typically occupies at zero pressure gradient. Experimental support for these hypotheses was found from the results of the first and second joint DLR/UniBw experiment, cf. Knopp et al. (2014b) and Knopp et al. (2021), and from the analysis of the data base in Coles and Hirst (1969), see Knopp (2016).

The status of work on the improvement of RANS models for turbulent boundary layers at adverse-pressure gradient is rare in the literature. One of the few attempts to modify k-ω-type turbulence models for APG was the proposal by Rao and Hassan (1998). Their idea was to modify the equation for the turbulent kinetic energy k, so that the modified model gives the sqrt-law behaviour for the mean velocity at APG. Rao and Hassan proposed to modify the model for the turbulent diffusion of k by taking into account an additional modeling term, which may be associated with the diffusion due to pressure fluctuations and which scales with the streamwise component of the mean pressure gradient. This idea was studied and modified in Knopp (2016) for the SST k-ω model by Menter (1994), and for the SSG/LRR-ω model by Eisfeld et al. (2016) in Knopp et al. (2018).

2 Wind-tunnel experiments

The experiments were performed in the Eiffel type atmospheric wind tunnel (AWM) of UniBw in Munich in the 22-m-long test section of cross section $1.8\,\mathrm{m} \times 1.8\,\mathrm{m}$.

Experimental set-up

The two experiments used a contour model, which was mounted on the side wall of the wind tunnel, to generate an APG region in its rear part, see figure 1. The first part of the APG region was a 0.75m long curved element, which was used in both experiments. In the DLR/UniBw exp. II (named RETTINA II), the focus region was on a flat plate of length 0.4m at an opening angle of $14.4°$ downstream of the first curved element. In the DLR/UniBw exp. III (named VicToria, after the corresponding DLR internal project), a second curved element was added and the focus region was on a flat plate of length 0.762 m at an opening angle of $18.6°$, where a thin separation region occurs. Both models are shown in figure 1. The flow parameters were changed by a variation of the flow velocity and by changing the model in the rear part.

Flow conditions

The streamwise pressure gradient is shown in figure 2 for the DLR/UniBw exp. II and in figure 3 for the DLR/UniBw exp. III.

For the DLR/UniBw exp II, some characteristic boundary layer parameters for $U_{\mathrm{e,ref}} = 28.13\,\mathrm{m/s}$ and $U_{\mathrm{e,ref}} = 43.29\,\mathrm{m/s}$ are given in table 1. The flow is remote from separation. For the DLR/UniBw exp. III, the boundary layer parameters are given for $U_{\mathrm{e,ref}} = 35.5\,\mathrm{m/s}$ in table 2. Flow separation occurs in the rear part of the flat plate.

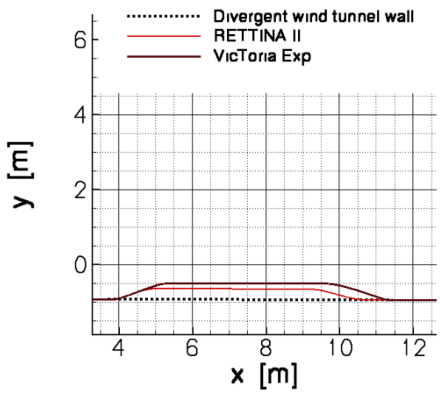

Figure 1: Sketch of DLR/UniBw exp. II (named RETTINA II) and of DLR/UniBw exp. III (named VicToria).

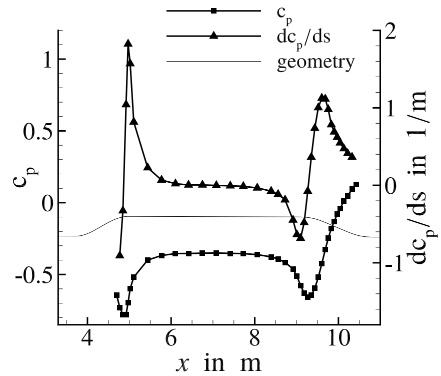

Figure 2: Distribution of c_p for the DLR/UniBw exp II.

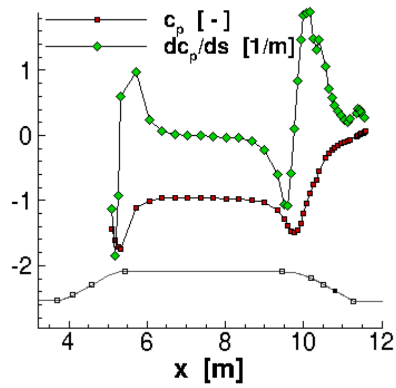

Figure 3: Distribution of c_p for the DLR/UniBw exp III.

Table 1: Characteristic boundary layer parameters for the DLR/UniBw exp. II at $U_{\mathrm{e,ref}} = 28.13\,\mathrm{m/s}$ and $U_{\mathrm{e,ref}} = 43.29\,\mathrm{m/s}$.

x in m	U_{e} in m/s	Re_θ	Re_τ	Δp_s^+	β_{RC}
8.12	28.13	24358	9304	-0.0002	-0.156
9.94	25.50	39822	6939	0.0185	27.06
8.12	43.29	35908	13214	-0.0001	-0.167
9.94	39.18	57363	9799	0.0114	26.37

Table 2: Characteristic boundary layer parameters for the DLR/UniBw exp. III at $U_{\mathrm{e,ref}} = 35.5\,\mathrm{m/s}$.

x in m	U_{e} in m/s	Re_θ	Re_τ	Δp_s^+	β_{RC}
8.63	35.5	22634	9308	-0.0004	-0.39
10.55	30.7	47576	4620	0.16	151.1

Measurement technique

For the measurement of the mean velocity and of the Reynolds stresses, different techniques were combined. A large scale overview measurement was applied in the centerplane using 2D2C particle image velocimetry (PIV) to measure the two components (2C) of streamwise and wall-normal velocity in the two dimensional (2D) plane of streamwise and wall-normal direction. Moreover, in the adverse pressure gradient region, different high-resolution particle-tracking velocimetry (PTV) and Lagrangian particle-tracking (LPT) approaches were applied, i.e., microscopic long-range microscope 2D2C-PTV and 3D3C-LPT. The wall-shear stress was measured using oil-film interferometry for both experiments. For details see Novara et al. (2016), Knopp et al. (2021), Knopp et al. (2018).

3 Wall-law at adverse pressure gradient

The aim is to find a wall-law for the mean velocity at APG. First the results for the DLR/UniBw experiments are considered. Then a data-base approach using a large number of wind-tunnel experiments in Coles and Hirst (1969) and DNS data is used.

Results from the DLR/UniBw experiments

From the two joint DLR/UniBw experiments, the following results for the mean velocity were found. The log-law in the mean velocity is a robust feature at APG. The log-law region is thinner than its zero pressure gradient counterpart, and does not extend up to the outer edge of the inner layer at $y = 0.2\delta_{99}$. The extent of the log-law region is decreasing with increasing Δp_s^+. A square-root law (or half-power law) emerges above the log-law in a large part of the region occupied by the log-law at zero pressure gradient.

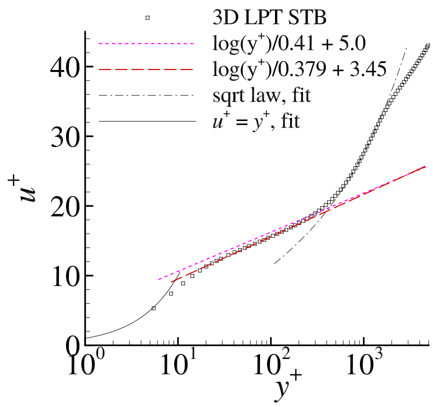

Figure 4: Mean velocity profile for the DLR/UniBw experiment II for at $x = 9.944\,\mathrm{m}$, $\Delta p_s^+ = 0.0114$ and $Re_\theta = 57363$ (note that $y^+ < 0.5\delta_{99}^+$ is shown).

Data-base study

The mean-velocity profiles of the data base Coles and Hirst (1969) were fitted in the inner layer by this wall-law. The wall-law consists of a log-law region in the inner part, and, above the log-law, a half-power law extending up to around $y = 0.2\delta_{99}$. This is shown for the flow by Schubauer and Klebanoff in figure 5.

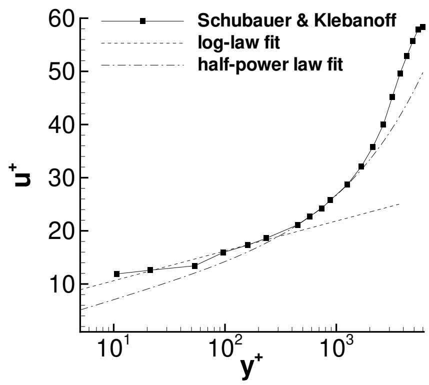

Figure 5: Mean velocity profile for flow 2134 by Schubauer & Klebanoff at $\Delta p_s^+ = 1.17 \times 10^{-2}$ and $Re_\theta = 53839$, see Coles and Hirst (1969).

Two characteristics of this wall law are the extent of the log-law region $y^+_{\mathrm{log,max}}$ and the intercept of the log-law and the square-root law y^+_{incpt}. The data indicate that both depend on the pressure gradient $\Delta p_s^+ = \nu/(\rho u_\tau^3)\mathrm{d}P/\mathrm{d}s$, on the Reynolds number $\delta^+ = Re_\tau$, and, as a higher-order effect, on the streamwise deceleration parameter $\Delta u^+_{\tau,s} = \nu/u_\tau^2 \mathrm{d}u_\tau/\mathrm{d}s$.

For $y^+_{\mathrm{log,max}}$, similar values were observed for different flows provided that Δp_s^+, $\Delta u^+_{\tau,s}$ and Re have

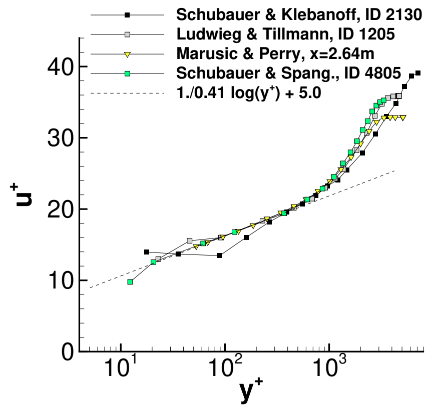

Figure 6: Mean velocity profiles at similar values of $\Delta p_s^+ \approx 0.0045$ and $\Delta u_{\tau,s}^+ \approx -8.7 \times 10^{-6}$.

similar values, see figure 6.

The values for y_{incpt}^+ found in the analysis of the mean-velocity profiles of the data-base are plotted as $y_{\text{incpt}}^+/(\delta^+)^{1/2}$ versus Δp_s^+ in figure 7. It is found that $y_{\text{incpt}}^+/(\delta^+)^{1/2}$ is slightly decreasing with increasing values of Δp_s^+. The range of Re_θ-values in the figure is large, varying from $Re_\theta = 900$ for the DNS by Manhart & Friedrich up to $Re_\theta = 95000$ for the flow by Perry. The scatter in the results is expected to be in part due to the uncertainty to determine y_{incpt}^+, δ, and u_τ, but could also depend on flow-physical parameters not accounted for in this simple model. An empirical correlation $y_{\text{incpt}}^+/(\delta^+)^{1/2} = 2.3(\Delta p_s^+)^{-0.2}$ is used as to approximate the data points.

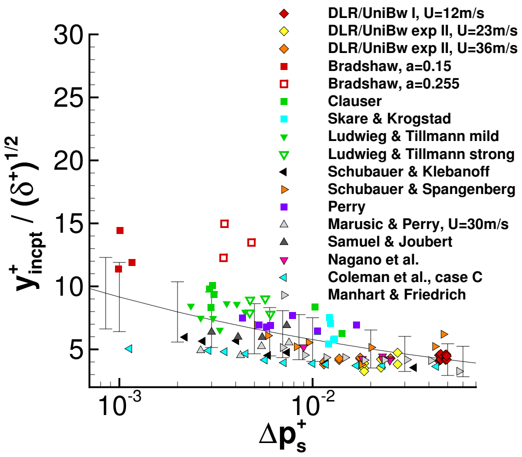

Figure 7: Data base analysis: y^+-position of the intercept between log-law and half-power law.

4 RANS turbulence modelling

For RANS turbulence modelling, the SSG/LRR-ω model is used. The transport equation for the Reynolds stresses $\overline{u_i'u_j'}$ can be written in the form

$$\frac{\partial}{\partial x_k}\left(U_k \overline{u_i'u_j'}\right) = P_{ij} + \Pi_{ij} - \epsilon_{ij} + D_{ij}^\nu + D_{ij}^t$$

Here P_{ij} denotes production, ϵ_{ij} denotes dissipation, and D_{ij}^ν and D_{ij}^t denote the viscous and turbulent transport of $\overline{u_i'u_j'}$, see Eisfeld et al. (2016). The corresponding equation for the turbulent kinetic energy $k = \frac{1}{2}\overline{u_i'u_i'}$ can be written as

$$\vec{\nabla} \cdot (\vec{U}k) = P_k - \epsilon + D_k^\nu + D_k^t \tag{1}$$

The equation for ω written in the form

$$\vec{\nabla} \cdot (\vec{U}\omega) - D_\omega^\nu - D_\omega^t = P_\omega - \epsilon_\omega \tag{2}$$

with viscous and turbulent diffusion terms D_ω^ν, D_ω^t, production term P_ω and dissipation term ϵ_ω.

Modification to account for the half-power law

The boundary layer analysis of the ω-equation at APG uses the assumption that there exists a half-power law region, where the mean velocity profile follows a sqrt-law and the total shear stress is growing as $\tau^+ = 1 + \lambda \Delta p_s^+ y^+$, $\lambda = 0.7$. This was described in Knopp (2016) and Knopp et al. (2018). It was shown that the ω-equation is not consistent with the assumed solution in the sqrt-law region at APG. From this analysis a model discrepancy term m_ω^+ for the sqrt-layer was inferred. The discrepancy term can be expressed using the pressure diffusion term D_k^p proposed for the k-equation by Rao and Hassan (1998). The pressure diffusion term for the ω-equation becomes

$$-D_\omega^p = -\frac{\omega}{k}\frac{\partial}{\partial x_j}\left(\sigma_{k,P}\nu_t \frac{\partial P}{\partial x_i}\frac{b_{ij}}{\rho}\right) \quad \text{if} \quad \Delta p_s^+ > 0 \tag{3}$$

and is set to zero for $\Delta p_s^+ \le 0$. Here for the anisotropy tensor b_{ij} the following definition is used

$$b_{ij} = \frac{\tau_{ij}}{\rho k} + \frac{2}{3}\delta_{ij}\,, \qquad \tau_{ij} = -\rho\overline{u_i'u_j'}. \tag{4}$$

The coefficients of the pressure diffusion term are

$$\sigma_{\omega,P} = \sigma_\omega \lambda \beta_k^{-1}\,, \quad \beta_k = 0.09\,, \quad \lambda = 0.7 \tag{5}$$

The pressure diffusion term is only activated in the assumed sqrt-law region. For this purpose, the blending functions f_{b2} and f_{b3} are used, which are described in detail in Knopp (2016). The modified ω-equation with the additional pressure diffusion term D_ω^p and with the blending functions f_{b2}, f_{b3} becomes

$$\vec{\nabla} \cdot (\vec{U}\omega) - D_\omega^\nu - D_\omega^t - f_{b2}f_{b3}D_\omega^p = P_\omega - \epsilon_\omega \tag{6}$$

The blending function f_{b2} describes the progressive breakdown of the log-law in APG. It accounts for the modelling hypothesis that the outer edge of the log-law region is decreasing with increasing Δp_s^+ and is based on y_{incpt}^+. The function f_{b2} has a value of zero in the near wall region and in the log-law region, increases in the transition region, and has a value of one in the sqrt-law region. On the other hand, the function f_{b3} has a value of one in the inner part of the boundary layer and goes down to zero for $y > 0.2\delta_{99}$.

5 Results of RANS simulations

DLR/UniBw moderate APG exp. II

For the DLR/UniBw moderate APG exp. II, the incoming turbulent boundary layer at the ZPG reference position $x = 8.12\,\mathrm{m}$ is matched by the RANS results, as shown here for the SSG/LRR-ω model in figure 8.

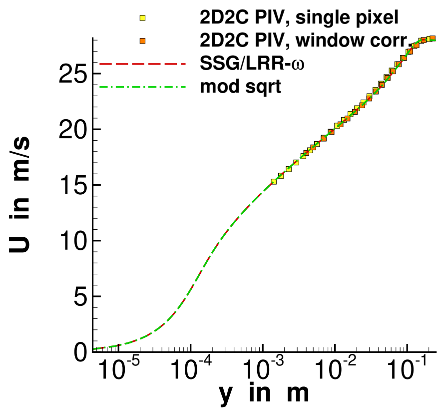

Figure 8: Exp. II, case $U_{\mathrm{e,ref}} = 28.1\,\mathrm{m/s}$: u^+ at $x = 8.12\,\mathrm{m}$ at the ZPG reference position.

In the APG region, the SSG/LRR-ω model overpredicts the mean velocity for $y < 0.05\delta_{99}$ in the inner layer, see figure 9. Using the sqrt-law modification, the mean velocity is reduced and becomes closer in agreement with the experimental data.

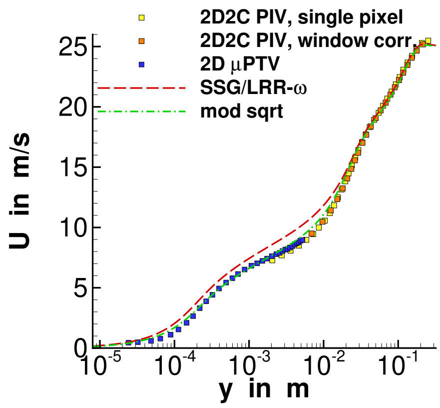

Figure 9: Exp. II, case $U_{\mathrm{e,ref}} = 28.1\,\mathrm{m/s}$: u^+ in the adverse pressure gradient region at $x = 9.944\,\mathrm{m}$.

The sqrt-law modification causes smaller values for c_f in the APG region, in better agreement with the experimental data by OFI and microscopic PTV, see figure 10.

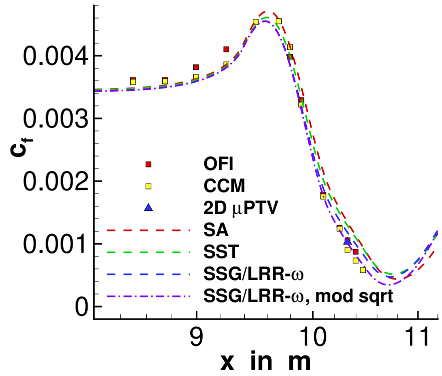

Figure 10: Exp. II, case $U_{\mathrm{e,ref}} = 28.1\,\mathrm{m/s}$: c_f-distribution.

DLR/UniBw strong APG exp. III

For the DLR/UniBw strong APG exp. III, the SA, SST, and SSG/LRR-ω model were also found to overpredict the mean velocity in the inner part of the inner layer in the APG region, see figure 11. Using the sqrt-law modification, the mean velocity is decreased and in closer agreement with the experimental data. Figure 11 shows u^+ in the APG region.

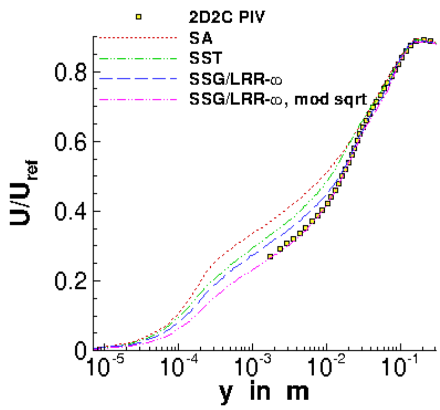

Figure 11: Exp. III, case $U_{\mathrm{e,ref}} = 35.5\,\mathrm{m/s}$: u^+ at $x = 10.41\,\mathrm{m}$ in the APG region.

The sqrt-law modification causes smaller values for c_f in the APG region, in better agreement with the OFI data, see figure 12.

6 Conclusions

A modification of the SSG/LRR-ω model for turbulent boundary flows in adverse pressure gradient based on a new wall law for the mean velocity at adverse pressure gradients was presented. It accounts for a half-power law region of the mean velocity in a part of the inner layer. The modification gives improved predictions for two DLR/UniBw turbulent boundary layer experiments at moderate and strong adverse pressure gradient without and with separation.

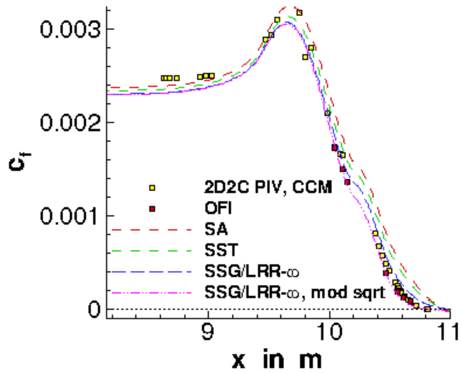

Figure 12: Exp. III, case $U_{\mathrm{e,ref}} = 35.5\,\mathrm{m/s}$: c_f-distribution.

Acknowledgments

The funding by the DLR aeronautical programm, by the institute AS, and by DFG (Grant KA 1808/14-1 and SCHR 1165/3-1) is gratefully acknowledged.

7 References

Alving, A. E. and Fernholz, H. H. Mean-velocity scaling in and around a mild, turbulent separation bubble. *Phys. Fluids*, 7:1956–1969, 1995.

Bush, R. H., Chyczewski, T. S., Duraisamy, K., Eisfeld, B., Rumsey, C. L., and Smith, B. R. Recommendations for future efforts in RANS modeling and simulation. 2019. AIAA Paper 2019-0317.

Coleman, G. N., Rumsey, C. L., and Spalart, P. R. Numerical study of turbulent separation bubbles with varying pressure gradient and Reynolds number. *J. Fluid Mech.*, 847:28–70, 2018.

Coles, D. E. and Hirst, E. A. *Computation of Turbulent Boundary Layers - 1968 AFOSR-IFP-Stanford Conference*. 1969.

Eisfeld, B., Rumsey, C., and Togiti, V. Verification and validation of a second-moment-closure model. *AAIA J.*, 54:1524–1541, 2016.

Johnstone, R., Coleman, G. N., and Spalart, P. R. The resilience of the logarithmic law to pressure gradients: evidence from direct numerical simulation. *J. Fluid Mech.*, 643:163–175, 2010.

Knopp, T. A new wall-law for adverse pressure gradient flows and modification of k-ω type RANS turbulence models. *AIAA Paper 2016-0588*, 2016.

Knopp, T., Schanz, D., Schröder, A., Buchmann, N. A., Cierpka, C., Hain, R., and Kähler, C. J. Experimental investigation of a turbulent boundary layer at adverse pressure gradient at Re_θ up to 10000 using large-scale and long-range microscopic particle imaging. In *WALLTURB Workshop: Progress in Wall Turbulence*, pages 271–281. Springer Netherlands, 2014a.

Knopp, T., Schanz, D., Schröder, A., Dumitra, M., Hain, R., and Kähler, C. J. Experimental investigation of the log-law for an adverse pressure gradient turbulent boundary layer flow at Re_θ up to 10000. *Flow, Turbul. Combust.*, 92:451–471, 2014b.

Knopp, T., Novara, M., Schanz, D., Geisler, R., Philipp, F., Schröder, A., Willert, C., and Krumbein, A. Modification of the SSG/LRR-omega RSM for turbulent boundary layers at adverse pressure gradient with separation using the new DLR VicToria experiment. In *Contributions to the 21th STAB/DGLR Symposium Darmstadt, Germany*. Springer, 2018.

Knopp, T., Reuther, N., Novara, M., Schanz, D., Schülein, E., Schröder, A., and Kähler, C. J. Experimental analysis of the log law at adverse pressure gradient. *J. Fluid Mech.*, 918:A17–1–A17–32, 2021.

Menter, F. R. Two-equation eddy-viscosity turbulence models for engineering applications. *AAIA J.*, 32: 1598–1605, 1994.

Novara, M., Schanz, D., Reuther, N., Kähler, C. J., and Schröder, A. Lagrangian 3D particle tracking in high-speed flows: Shake-The-Box for multi-pulse systems. *Exp. Fluids*, 57:128 1–20, 2016.

Perry, A. E., Bell, J. B., and Joubert, P. N. Velocity and temperature profiles in adverse pressure gradient turbulent boundary layers. *J. Fluid Mech.*, 25: 299–320, 1966.

Rao, M. S. and Hassan, H. A. Modeling turbulence in the presence of adverse pressure gradients. *J. Aircraft*, 35:500–502, 1998.

Schatzman, D. M. and Thomas, F. O. An experimental investigation of an unsteady adverse pressure gradient turbulent boundary layer: embedded shear layer scaling. *J. Fluid Mech.*, 815:592–642, 2017.

Slotnick, J., Khodadoust, A., Alonso, J., Darmofal, D., Gropp, W., Lurie, E., and Mavriplis, D. CFD Vision 2030 Study: A Path to Revolutionary Computational Aerosciences. Technical report, NASA/CR2014-218178, 2014.

Telbany, M. M. M. E. and Reynolds, A. J. Velocity distributions in plane turbulent channel flows. *J. Fluid Mech.*, 100:1–29, 1980.